

Perturbation theory of angular molecules interacting through the Kihara potential

Carlos Vega and Santiago Lago

Departamento de Química Física, Facultad de Ciencias Químicas, Universidad Complutense de Madrid, 28040-Madrid, Spain

(Received 8 August 1990; accepted 4 September 1990)

A perturbation theory for angular molecules interacting through the Kihara potential is proposed. The theory is applied to a model of propane and the different approximations of the theory are checked by comparing the theoretical with previously obtained simulation results. We also obtained vapor-liquid equilibria of propane by fitting the potential parameters with the theory. Good agreement between theoretical and experimental results was obtained. Thus, the Kihara potential which is much simpler than the site-site model for this kind of molecule is able to represent the equilibrium behavior of angular nonpolar molecules.

I. INTRODUCTION

Angular molecules, as propane, are of high interest for industrial purposes. The effort to understand thermodynamic properties of propane from a microscopic point of view has been devoted to simulation studies¹⁻³ and to the development of perturbation theories.⁴ In the cases, the potential model used was the site-site Lennard-Jones (12-6). Two conclusions can be drawn from these studies. The first is that the site-site potential model is a good effective pair potential for propane as it has been shown from the simulation studies. The second is that the perturbation scheme proposed by Fischer⁵ and extended to propane by Lustig⁴ can yield good agreement with experimental results if the potential parameters are fitted within the framework of the theory. However, the situation is not completely satisfactory in three respects. First, the theory systematically gives too high pressures at high densities. Second, the potential parameters are obtained using the theory and, therefore, they compensate the theoretical errors and partially lose their physical meaning. Third, the theory can only be improved if a systematic study of the reference system is carried out. Unfortunately, this is an extremely difficult task when the Weeks, Chandler, and Andersen (WCA)-like division of the potential⁶ is applied to the full pair potential. Therefore, although the search for better potential parameters within the site-site model of propane can be continued and improvement can be expected, this improvement of the perturbation scheme is difficult by itself due to the difficulties involved in the simulation of the reference system.

On the other hand, Kihara proposed some time ago⁷ a potential model in which the pair interaction depends on the shortest distance ρ between the molecular cores. These cores are chosen to represent the molecular shape approximately. Several simulation studies have been recently performed for this model in linear^{8,9} and nonlinear molecules.¹⁰ These studies have shown that the Kihara potential is a good effective pair potential and can compete with the site-site model. Moreover, the comparison of Kihara and site-site model potentials with *ab initio* results for some relative orientations of propane revealed the superiority of the Kihara model over the site-site.¹⁰ Therefore, there are good reasons to continue with the theoretical study of the Kihara potential using per-

turbation theories. Recently, two studies of this type^{11,12} have appeared. The first one extends the perturbation theory of Fischer to linear molecules interacting through the Kihara potential. The second uses the formalism of the average surface-surface correlation function. Again, systematic deviations from experimental results were found when the perturbation scheme of Fischer was applied to linear Kihara molecules.¹¹ However, the situation is now better than with the site-site model because the reference system can be studied systematically through simulation.^{9,10,13} The different approximations of the theory can be checked one by one, and that allows a systematic improvement of the theory. We have already worked with linear molecules in that direction¹³ showing that the main failure of the theory comes from neglecting the orientational dependence of the background correlation function $\gamma(r_{12}, \omega_1, \omega_2)$. The goal of this work is threefold. The first aim is to extend Fischer's perturbation scheme to nonlinear molecules interacting through the Kihara potential and to apply the theory to a previously studied model of propane.¹⁰ The second goal is to test the different approximations made in the theory by comparing the theoretical values of the first perturbation terms A_0 , A_1 , and A_2 with the values obtained by simulation. We shall show that a good description of the three perturbation terms is achieved, although at high densities a more elaborated approximation to get the structure of the reference fluid is needed. The third purpose is to see whether one can obtain a good description of the behavior of real propane, using the Kihara potential along with perturbation theory as long as the potential parameters are obtained from fitting theoretical to experimental results.

With this study we try to show that the Kihara model can give results similar in accuracy to those obtained from the site-site one, for small nonpolar molecules, as propane.

The scheme of the paper is as follows: in Sec. II we shall describe in detail the theory used. In Sec. III, we show the numerical procedure used in the calculations. Section IV is devoted to checking one by one the different approximations of the theory by comparing theoretical with previously obtained MD results of the model. In Sec. V, we apply the theory to propane and a comparison with experimental results is given. Finally, Sec. VI gives the main conclusions.

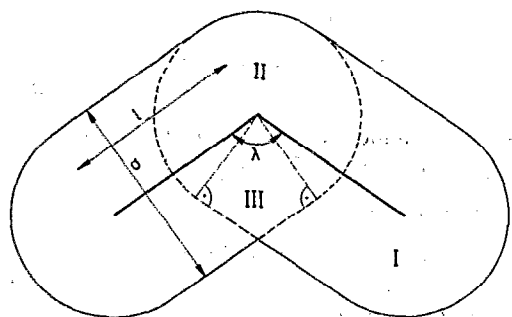


FIG. 1. Geometry of the Kihara model of propane. The core is made up by two fused, hard rods which form an angle λ . Roman numbers refer to the regions defined in the Appendix. These regions are separated by dashed lines.

II. THEORY

The potential model used in this work and which will be denoted as Kihara model for angular molecules is given by¹⁰

$$u(\rho) = 4\epsilon[(\sigma/\rho)^{12} - (\sigma/\rho)^6] \quad (1)$$

$$\rho = \text{minimum}(\rho_{11}, \rho_{12}, \rho_{21}, \rho_{22}) \quad (2)$$

ρ_{ij} = shortest distance between (rod_{*i*} of molecule 1

$$\text{— rod}_j \text{ of molecule 2}), \quad (3)$$

where ρ is the minimum distance between molecular cores. The molecular core is given by two connected rods for angular molecules (see Fig. 1) and, therefore, the shortest distance between the cores, is the minimum between the four rod-rod shortest distances.

The division of the full pair potential into reference u_0 and perturbation part u_1 is given by¹⁴

$$u_0 = u(r_{12}, \omega_1, \omega_2) - u_{\min}(\omega_1, \omega_2) \quad r_{12} < r_{12\min}(\omega_1, \omega_2), \quad (4)$$

$$u_0 = 0 \quad r_{12} > r_{12\min}(\omega_1, \omega_2), \quad (5)$$

$$u_1 = u_{\min}(\omega_1, \omega_2) \quad r_{12} < r_{12\min}(\omega_1, \omega_2), \quad (6)$$

$$u_1 = u(r_{12}, \omega_1, \omega_2) \quad r_{12} > r_{12\min}(\omega_1, \omega_2), \quad (7)$$

where r_{12} is the distance between molecular centers of mass and $r_{12\min}(\omega_1, \omega_2)$ is the value of r_{12} at which a minimum in the pair potential for a given orientation (ω_1, ω_2) is achieved. $u_{\min}(\omega_1, \omega_2)$ is the potential value at the minimum. When division given by Eqs. (4)–(7) is applied to the potential of Eqs. (1)–(3) one obtains¹¹

$$u_0 = u(r_{12}, \omega_1, \omega_2) + \epsilon \quad \rho < 2^{1/6}\sigma, \quad (8)$$

$$u_0 = 0 \quad \rho > 2^{1/6}\sigma, \quad (9)$$

$$u_1 = -\epsilon \quad \rho < 2^{1/6}\sigma, \quad (10)$$

$$u_1 = u(r_{12}, \omega_1, \omega_2) \quad \rho > 2^{1/6}\sigma. \quad (11)$$

The residual Helmholtz free energy A of the system can be expanded around that of the reference system A_0 to give¹⁵

$$\frac{A}{NkT} = \frac{A_0}{NkT} + \frac{A_1}{NkT} + \frac{A_2}{NkT}, \quad (12)$$

where the first and the second order perturbation terms A_1

and A_2 are, respectively, given by

$$A_1/N = n/2 \int u_1(r_{12}, \omega_1, \omega_2) g_0(r_{12}, \omega_1, \omega_2) \times d\mathbf{r}_{12} d\omega_1 d\omega_2 = \langle U_1 \rangle_0, \quad (13)$$

$$U_1 = \sum_{i < j} u_1(i, j), \quad (14)$$

$$A_2 = -1/(2kT) (\langle U_1^2 \rangle_0 - \langle U_1 \rangle_0^2), \quad (15)$$

where brackets with subscript 0 stand for canonical ensemble average over the reference system and $g_0(r_{12}, \omega_1, \omega_2)$ is the pair correlation function of the reference system. The numerical density of the system is given by n . Thus, to obtain A in Eq. (12), it is necessary to know the structure and the thermodynamic properties of the reference system. Fischer⁵ and later Lüstig⁴ proposed a perturbation scheme consisting of the following steps:

(1) A BLIP expansion¹⁶ of a hard system u_H around the soft repulsive system u_0 is made. In this expansion either the site-site distance (in the site-site model) or the rod length (in the Kihara model) is kept constant. The diameter of the hard equivalent body at every density and temperature is found by setting to zero the first order term in the BLIP expansion:

$$n/2 \int [\exp(-\beta u_0) - \exp(-\beta u_H)] \times y_0(r_{12}, \omega_1, \omega_2) d\mathbf{r}_{12} d\omega_1 d\omega_2 = 0 \quad (16)$$

so that the residual Helmholtz free energy of the reference system can be written to first order of the BLIP expansion as

$$A_0 = A_H, \quad (17)$$

where A_H is the residual Helmholtz free energy of the corresponding hard body.

(2) A_H can be obtained from any of the available equations of state (EOS) proposed for hard convex bodies.¹⁷ We shall use three of these EOS in this work. All of them can be written in a general form as

$$Z_H = \frac{pV}{NkT} = \frac{(1 + k_1\eta + k_2\eta^2 + k_3\eta^3)}{(1 - \eta)^3} \quad (18)$$

$$\eta = nV_H. \quad (19)$$

The value of the constants k_1 , k_2 , and k_3 for the different equations of state^{18–20} are given in Table I. These constants are always related to the nonsphericity parameter α defined by

$$\alpha = (R_H S_H)/(3V_H), \quad (20)$$

TABLE I. Values of the parameters k_1 , k_2 , and k_3 of Eq. (18) of the text for three different EOS of hard convex bodies.

EOS	k_1	k_2	k_3
ISPT ^a	$(3\alpha - 2)$	$(3\alpha^2 - 3\alpha + 1)$	$-\alpha^2$
Nezbeda ^b	$(3\alpha - 2)$	$(\alpha^2 + \alpha - 1)$	$-\alpha(5\alpha - 4)$
Boublik ^c	$(3\alpha - 2)$	$(3\alpha^2 - 3\alpha + 1)$	$-\alpha(6\alpha - 5)$

^a Reference 18.

^b Reference 19.

^c Reference 20.

where R_H , S_H , and V_H stand for the mean radius of curvature, the surface, and the volume of the molecule, respectively. The residual Helmholtz free energy of the hard system can be obtained from integration of Eq. (18) to obtain

$$A_H/NkT = \frac{\eta(c_1 + c_2\eta)}{(1-\eta)^2} + c_3 \ln(1-\eta), \quad (21)$$

$$c_1 = (k_1 - k_3 + 2), \quad (22)$$

$$c_2 = (3k_3 + k_2 - k_1 - 3)/2, \quad (23)$$

$$c_3 = -(k_3 + 1). \quad (24)$$

The mean radius of curvature R_H is well defined for convex shapes,²¹ and therefore, α is uniquely defined for convex bodies. Indeed, the hard body corresponding to the Kihara angular model (see Fig. 1) is not convex. Therefore, if we wish to use any of the proposed EOS for hard convex fluids we have to define α . We have examined two possibilities.

(2a) To evaluate the actual value of the volume V_H and surface S_H of the hard body and to take R_H from a convex body of shape close to the molecular shape.⁴ For angular molecules a reasonable choice of this close convex body could be that of the parallel body to the triangle made up by the two rods. Details of the evaluation of S_H and V_H for angular hard models as well as the well known formula of R_H for the parallel body of a triangle are given in the Appendix.

(2b) To obtain α by identifying the second virial coefficient of the hard nonconvex molecule B_{2H} with that one of a convex body of nonsphericity given by α as was done in Ref. 22, i.e.,

$$B_{2H}/V_H = (1 + 3\alpha). \quad (25)$$

Both choices of α [(2a) and (2b)] have been considered in this work and a discussion of the results is given in the next section. Thus, Eqs. (17)–(24) can be used to determine the properties of the reference system.

The evaluation of the perturbation terms A_1 and A_2 also requires the knowledge of the structure of the reference system. Although considerable progress has been achieved during the last few years in the solution of integral equations for anisotropic linear models,^{23–25} very little has been done for nonlinear models. The majority of the structural studies of nonlinear molecules are based on the solution of the site–site Ornstein–Zernike (SSOZ) equation for multisite models.²⁶ The SSOZ presents the disadvantage that can only be applied to site–site fluids. Simple models based on Gaussian²⁷ or Kihara potentials are out of the applicability of the SSOZ. Furthermore, the solution of the Ornstein–Zernike equation (OZ) for hard nonlinear models would need a great amount of computer time and perturbation theory based on this solution would be a long time procedure, thus losing its simplicity. Therefore, a compromise between accuracy and simplicity is needed to obtain the structure of the reference system. Reference average Mayer function (RAM) theory¹⁶ provides such a compromise and will be used as explained in point (3).

(3) The structure of the reference system will be obtained from a zero order approximation of the background correlation function of the reference system $y_0(r_{12}, \omega_1, \omega_2)$

around a spherical RAM potential $\Phi_{RAM}(r_{12})$ defined by¹⁶ $\exp[-\beta\Phi_{RAM}(r_{12})] = \langle \exp[-\beta u_0(r_{12}, \omega_1, \omega_2)] \rangle_g$, (26)

where the subscript g stands for geometrical average. The zero order approach to $y_0(r_{12}, \omega_1, \omega_2)$ is given by

$$y_0(r_{12}, \omega_1, \omega_2) = y_{RAM}(r_{12}), \quad (27)$$

where $y_{RAM}(r_{12})$ is the background correlation function of the system interacting through $\Phi_{RAM}(r_{12})$. With the approximation of Eq. (27), $g_0(r_{12}, \omega_1, \omega_2)$ is given by

$$g_0(r_{12}, \omega_1, \omega_2) = \exp[-\beta u_0(r_{12}, \omega_1, \omega_2)] y_{RAM}(r_{12}). \quad (28)$$

According to Eq. (28) the radial distribution function of the reference system $G_0(r_{12})$ is given by

$$G_0(r_{12}) = \langle g_0(r_{12}, \omega_1, \omega_2) \rangle_g = G_{RAM}(r_{12}), \quad (29)$$

and using Eqs. (13) and (28), A_1 can be written as

$$A_1/N = 2n\pi \int_0^\infty \langle u_1 \exp(-\beta u_0) \rangle_g \times y_{RAM}(r_{12}) r_{12}^2 dr_{12}. \quad (30)$$

(4) the OZ equation for the potential $\Phi_{RAM}(r_{12})$

$$h(r_{12}) = c(r_{12}) + n \int c(r_{13}) h(r_{23}) dr_{13}, \quad (31)$$

along with either the Percus–Yevick (PY) or the reference hypernetted chain (RHNC) closure relations¹⁵

$$c(r_{12}) = [1 + h(r_{12})] \{1 - \exp[-\beta u(r_{12})]\} \quad (\text{PY}) \quad (32)$$

$$c(r_{12}) = h(r_{12}) - B_{HS}(r_{12}) - \beta u(r_{12}) - \ln[h(r_{12}) + 1] \quad (\text{RHNC}), \quad (33)$$

must be solved to obtain $y_{RAM}(r_{12})$. Here $c(r_{12})$ is the direct correlation function and $h(r_{12})$ is the total correlation function. In the case of the RHNC, the bridge function $B_{HS}(r)$ is taken to be equal that of a system of hard spheres whose diameter d_{HS} is given by²⁸

$$\int_0^\infty [G_{RAM}(r_{12}) - G_{HS}(r_{12})] \frac{dB_{HS}(r_{12})}{dd_{HS}} dr_{12} = 0. \quad (34)$$

Examples of the shape of the potential $\Phi_{RAM}(r_{12})$ for several systems and a discussion of the quality of PY and RHNC approximations for this potential can be found in Ref. 13.

(5) The A_2 term involves the correlation functions of two, three, and four particles of the reference system and its exact evaluation is very difficult.¹⁶ We shall use a generalization of the Barker–Henderson approximations²⁹ (macroscopic compressibility and local compressibility) to nonspherical fluids. These approximations were already used by Boublik for nonspherical fluids.¹² Thus, we approximate A_2 by

$$A_2/NkT = -\frac{\pi n}{kT} \left(\frac{\delta n}{\delta p} \right)_0 \int_0^\infty \langle u_1^2 \exp(-\beta u_0) \rangle_g \times y_{RAM}(r_{12}) r_{12}^2 dr_{12}. \quad (35)$$

$$A_2/NkT = -\frac{\pi n}{kT} \left(\frac{\delta n}{\delta p} \right)_0 \frac{\delta}{\delta n} n \int_0^\infty \langle u_1^2 \exp(-\beta u_0) \rangle_g \times y_{RAM}(r_{12}) r_{12}^2 dr_{12}. \quad (36)$$

Equations (35) and (36) are called the macroscopic (m.c) and the local compressibility (l.c) approximations, respectively. Equation (12), Eqs. (17)–(25), Eq. (30), and Eqs. (35) and (36) constitute the perturbation scheme of this work. Different variants of the theory can be obtained from:

- Using different EOS for the hard body system.
- Using any of the two available choices of α .
- Using PY [$y_{\text{RAM}}^{\text{PY}}(r_{12})$] or RHNC [$y_{\text{RAM}}^{\text{RHNC}}(r_{12})$] to obtain $y_{\text{RAM}}(r_{12})$, which is present in the integrals of A_1, A_2 , and in the BLIP condition [Eq. (16)].
- Using m.c or l.c to obtain A_2 .
- Using either first or second order perturbation theory.

The equation of state and the residual internal energy U can be obtained from the classical formulas

$$Z = 1 + \left(\frac{\partial A / NkT}{\partial n^*} \right)_T n^* \quad (37)$$

$$U / Nk = \left(\frac{\partial A / NkT}{\partial 1/T} \right)_n, \quad (38)$$

where $n^* = n\sigma^3$ stands for the reduced density. Assuming that the structure of the reference system is very close to the structure of the full potential, we can write the residual internal energy as

$$U / N = 2\pi n \int \langle u \exp(-\beta u_0) \rangle_g y_{\text{RAM}}(r_{12}) r_{12}^2 dr_{12}. \quad (39)$$

Finally, the vapor–liquid equilibria can be studied, treating the liquid phase by using perturbation theory and the gaseous phase by using the virial series up to the second virial coefficient B_2 (a good approximation for $T/T_c < 0.8$). The density of the liquid ρ_l and of the gas ρ_g coexisting at every temperature can be obtained by solving the system of nonlinear equations

$$\rho_l Z_l = (1 + B_2 \rho_g) \rho_g \quad (40)$$

$$A_l / NkT + Z_l + \ln(\rho_l) = B_2 \rho_g + (1 + B_2 \rho_g) + \ln(\rho_g). \quad (41)$$

For $T/T_c > 0.8$ more virial coefficients are needed to describe the gas phase. In this range of temperatures it is also possible to treat liquid and vapor phase by perturbation theory and to determine the equilibrium condition in a Gibbs (G, p) diagram as previously reported.¹¹

III. NUMERICAL DETAILS

The theory described in Sec. II needs the evaluation of several angular geometrical averages. All these averages have been computed by using the method of numerical integration proposed by Conroy.³⁰ Unidimensional integrals were calculated by using Simpson's rule. The evaluation of the shortest distance between rods have been described in detail elsewhere.^{31,32} The solution of OZ equation for the spherical potential $\Phi_{\text{RAM}}(r_{12})$ was carried out by using the efficient algorithm proposed by Labik and Malijevsky.³³ We have used 512 points and the grid width was of 0.0125σ . Fast Fourier transform was used to carry out conversion between real and reciprocal space. When the RHNC closure relation was used [Eq. (33)], the Labik and Malijevsky parameterization of the bridge function of hard spheres was used.^{34,35} The solution of the OZ for a given temperature and density spends about 15 s (PY) and 60 s (RHNC) in a IBM PS/2 80-041 with an INTEL 80387 mathematical coprocessor. Nevertheless, the calculation of the averages were the most time consuming. For instance, the orientational averages for 512 values of r_{12} at eight different temperatures were calculated in about 6 h with the same computer. The phase diagram of an angular substance as propane was determined in 8 h of computer real time. Therefore, the problem falls within the limits of applications of personal computers.

In the next section, we shall compare the results obtained from the theory described in Sec. II with the results obtained from molecular dynamics (MD) for a Kihara model of propane.¹⁰ Thus, all the approximations of Sec. II are separately checked.

TABLE II. Compressibility factors of the reference system of a Kihara model of propane (see first line of Table IX for the molecular parameters used) as obtained from (Ref. 10) and from the PT of this work by using three different EOS. α , which is also given in the last column was obtained from geometrical considerations. PY approximation was used to represent y_{RAM} . T^* is the reduced temperature $T^* = T/(\epsilon/k)$ and $n^* = n\sigma^3$.

T^*	n^*	Z_{MD}^a	Z_{ISPT}^b	Z_{NEZBEDA}^c	Z_{ROUHLIK}^d	α
0.5875	0.10	1.73	1.79	1.79	1.79	1.1418
0.5875	0.15	2.45	2.45	2.44	2.44	
0.5875	0.20	3.36	3.40	3.36	3.36	
0.5875	0.25	4.65	4.79	4.71	4.71	
0.5875	0.30	6.58	6.87	6.70	6.69	
0.5875	0.35	9.44	10.1	9.74	9.72	
0.5875	0.45	20.86	24.11	22.59	22.4	1.1422
0.8125	0.10	1.73	1.77	1.77	1.77	1.1436
0.8125	0.20	3.26	3.29	3.26	3.25	
0.8125	0.25	4.51	4.58	4.52	4.51	
0.8125	0.35	8.95	9.41	9.10	9.07	
0.8125	0.40	12.75	14.01	13.31	13.30	1.1440

^a Reference 10.

^b Reference 18.

^c Reference 19.

^d Reference 20.

TABLE III. Same as in Table II but α was obtained from the second virial coefficient of the equivalent hard system [Eq. (25) of the text].

T^*	n^*	Z_{MD}^a	Z_{ISPT}^b	$Z_{NEZBEDA}^c$	$Z_{BOUBLIK}^d$	α
0.5875	0.10	1.73	1.77	1.77	1.77	1.1119
0.5875	0.15	2.45	2.41	2.41	2.41	
0.5875	0.20	3.36	3.33	3.31	3.31	
0.5875	0.25	4.65	4.67	4.62	4.61	
0.5875	0.30	6.58	6.68	6.56	6.54	
0.5875	0.35	9.44	9.78	9.52	9.49	
0.5875	0.45	20.86	23.23	22.08	21.92	1.1127
0.8125	0.10	1.73	1.75	1.75	1.75	1.1141
0.8125	0.20	3.26	3.22	3.20	3.20	
0.8125	0.25	4.51	4.47	4.42	4.42	
0.8125	0.35	8.95	9.12	8.89	8.86	
0.8125	0.40	12.75	13.54	13.06	13.00	1.1148

^a Reference 10.^b Reference 18.^c Reference 19.^d Reference 20.TABLE IV. Same as in Table II using y_{RAM} as obtained from RHNC approximation.

T^*	n^*	Z_{MD}^a	Z_{ISPT}^b	$Z_{NEZBEDA}^c$	$Z_{BOUBLIK}^d$	α
0.5875	0.10	1.73	1.79	1.79	1.79	1.1418
0.5875	0.15	2.45	2.45	2.44	2.44	
0.5875	0.20	3.36	3.40	3.36	3.36	
0.5875	0.25	4.65	4.78	4.70	4.70	
0.5875	0.30	6.58	6.85	6.68	6.67	
0.5875	0.35	9.44	9.93	9.58	9.56	
0.5875	0.45	20.86	23.99	22.48	22.29	1.1424
0.8125	0.10	1.73	1.77	1.77	1.77	1.1437
0.8125	0.20	3.26	3.29	3.25	3.25	
0.8125	0.25	4.51	4.55	4.49	4.49	
0.8125	0.35	8.95	9.35	9.04	9.02	
0.8125	0.40	12.75	13.90	13.27	13.22	1.1442

^a Reference 10.^b Reference 18.^c Reference 19.^d Reference 20.TABLE V. Same as in Table III but using RHNC equation to represent y_{RAM} .

T^*	n^*	Z_{MD}^a	Z_{ISPT}^b	$Z_{NEZBEDA}^c$	$Z_{BOUBLIK}^d$	α
0.5875	0.10	1.73	1.77	1.77	1.77	1.1119
0.5875	0.15	2.45	2.41	2.41	2.41	
0.5875	0.20	3.36	3.33	3.31	3.31	
0.5875	0.25	4.65	4.66	4.61	4.60	
0.5875	0.30	6.58	6.66	6.54	6.53	
0.5875	0.35	9.44	9.62	9.36	9.33	
0.5875	0.45	20.86	23.11	21.98	21.81	1.1129
0.8125	0.10	1.73	1.75	1.75	1.75	1.1141
0.8125	0.20	3.26	3.22	3.20	3.20	
0.8125	0.25	4.51	4.45	4.40	4.40	
0.8125	0.35	8.95	9.07	8.84	8.81	
0.8125	0.40	12.75	13.44	12.96	12.90	1.1148

^a Reference 10.^b Reference 18.^c Reference 19.^d Reference 20.

TABLE VI. Values of the first order perturbation term as obtained from MD (Ref. 10) and from PT for the angular model of propane (see first line of Table IX for the potential parameters). PY and RHNC were used to represent y_{RAM} . The pair interaction was cut at r_c to evaluate A_1 in the simulations and in the theoretical results.

T^*	n^*	r_c/σ	A_1^{MD}/NkT	A_1^{PY}/NkT	A_1^{RHNC}/NkT
0.5875	0.10	5.13	-1.73	-1.72	-1.72
0.5875	0.15	4.48	-2.77	-2.75	-2.76
0.5875	0.20	4.07	-3.97	-3.89	-3.90
0.5875	0.25	3.78	-5.28	-5.12	-5.13
0.5875	0.30	3.56	-6.67	-6.39	-6.39
0.5875	0.35	3.38	-8.11	-7.70	-7.66
0.5875	0.45	3.11	-10.90	-10.23	-10.09
0.8125	0.10	5.13	-1.25	-1.25	-1.26
0.8125	0.20	4.07	-2.88	-2.83	-2.84
0.8125	0.25	3.78	-3.81	-3.71	-3.71
0.8125	0.35	3.38	-5.83	-5.56	-5.54
0.8125	0.40	3.23	-6.85	-6.49	-6.43

IV. THEORY VS SIMULATION

In a previous work¹⁰ we showed a MD study of a Kihara model of propane. We also simulated the reference system described by Eqs. (8) and (9) and, therefore, we were able to evaluate the thermodynamic behavior of this system as well as the perturbation terms A_1 and A_2 . We shall compare now, term by term, the theoretical with the numerical (MD) results of the model.

Let us start with the differential counterpart of Eq. (17) written as

$$\left(\frac{\partial A_0/NkT}{\partial n^*}\right)_T = \left(\frac{\partial A_H/NkT}{\partial n^*}\right)_T, \quad (42)$$

which is equivalent to

$$Z_0 = 1 + \left(\frac{\partial A_H[\alpha(n^*), \eta(n^*)]/NkT}{\partial n^*}\right)_T n^*. \quad (43)$$

Different possibilities to represent the reference system with the basic Eq. (43) arise from using a different EOS, from using a different choice of α , or from using $y_{\text{RAM}}(r_{12})$ as given by either the PY or RHNC approaches. Tables II to V show the results obtained from the different variants of the theory along with the results obtained from simulation. First, we observe that α as given by the second virial coefficient is always smaller than α from geometrical consider-

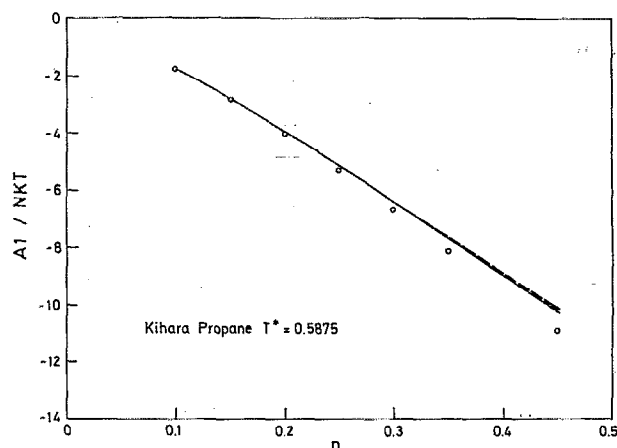


FIG. 2. A_1 as obtained from MD (dots), PT with y_{RAM} from PY (solid line) and PT with y_{RAM} from RHNC (dashed line).

ations. Similar behavior was found for different nonconvex models.¹⁷ Boublik EOS gives the best results and a good description of the reference system is achieved when used along with either α from geometrical considerations and $y_{\text{RAM}}^{\text{RHNC}}$ (see Table IV) or with α from the second virial coefficient and $y_{\text{RAM}}^{\text{PY}}$ (see Table III). In this work, we shall use this last option to describe the reference system because $y_{\text{RAM}}^{\text{PY}}$ is easier to obtain than $y_{\text{RAM}}^{\text{RHNC}}$. We should remark that, although the RHNC theory is by far superior to the PY theory to obtain $y_{\text{RAM}}(r_{12})$, as was proven for several RAM potentials,¹³ the inclusion of RHNC values in the integrand of Eq. (30) improves only very slightly the description of the reference system. Probably, only when the orientational dependence of the background correlation function is considered, the superiority of RHNC over PY will be manifest.

Let us now analyze the first order perturbation term A_1 . Table VI and Fig. 2 show the comparison between the theory and the pseudoexperimental data. The evident conclusion from this table is that although the agreement between theory and experiment is good at low densities, neither $y_{\text{RAM}}^{\text{PY}}$ nor $y_{\text{RAM}}^{\text{RHNC}}$ are able to reproduce A_1 at high densities. The theoretical values of A_1 are systematically less negative than the experimental ones at high densities. At high densities the values of A_1 obtained from PY are slightly better than the values of A_1 from RHNC although the differences are always

TABLE VII. Second order perturbation term as obtained from (Ref. 10) and from the theory for a Kihara propane like model (see first line of Table IX for the potential parameters).

T^*	n^*	A_2^{MD}/NkT	A_2/NkT^a	A_2/NkT^b	A_2/NkT^c	A_2/NkT^d
0.5875	0.10	-0.285	-0.287	-0.357	-0.288	-0.353
0.5875	0.45	-0.101	-0.057	-0.074	-0.055	-0.071
0.8125	0.10	-0.126	-0.157	-0.191	-0.158	-0.192
0.8125	0.20	-0.145	-0.147	-0.202	-0.148	-0.203
0.8125	0.40	-0.058	-0.052	-0.072	-0.052	-0.069

^a PY and macroscopic compressibility approximation.

^b PY and local compressibility approximation.

^c RHNC and macroscopic compressibility approximation.

^d RHNC and local compressibility approximation.

TABLE VIII. Reduced densities at zero pressure for two isotherms of the Kihara propane model (first line of Table IX) as obtained from MD (Ref. 10) and from first order perturbation theory. Boublik EOS equation of state along with α from the second virial coefficient of the hard model were used to obtain thermodynamic properties of the reference system.

T^*	MD	PY	RHNC
0.5875	0.371	0.352	0.345
0.8125	0.287	0.277	0.273

small. The main reason for the discrepancies between theory and simulation arises from the approximation of Eq. (27). Better results cannot be expected as long as the background correlation function of the reference system is approached by a spherical function. Similar conclusions were already obtained for a linear model.¹³ We conclude that Eq. (27) introduces a systematic error in the evaluation of A_1 , in the Kihara potential model of linear as well as angular molecules. Any improvement of the theory should incorporate orientational dependence in the background correlation function of the reference system.

Now let us analyze the second order perturbation term A_2 . Results are shown in Table VII. By comparing the simulation values of A_1 and A_2 at high densities, the fast convergence of the perturbation expansion is shown. That suggests that first order perturbation theory yields good results at high densities, but a second order theory is necessary at intermediate densities. Our results show that the obtained value of A_2 is slightly sensitive to the choice (PY or RHNC) of $y_{RAM}(r_{12})$. Macroscopic compressibility approximation works better than the local compressibility one. The agreement between the theoretical and the experimental values is only semiquantitative.

Once the term by term analysis of the theory has been done, let us check the accuracy of the global behavior. For this purpose we shall compare the density at zero pressure

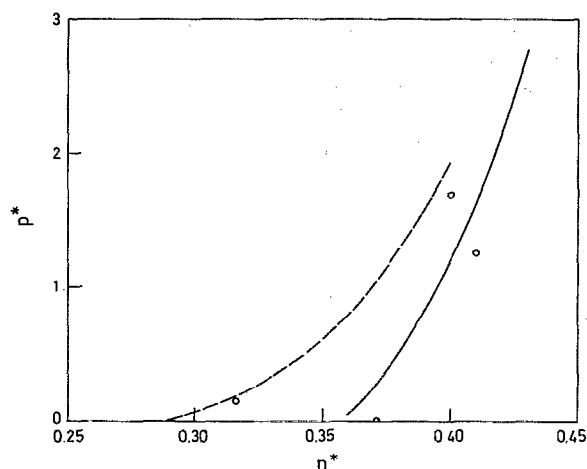


FIG. 3. Reduced pressure [$p^* = p/(kT/\sigma^3)$] of the propane model as function of the reduced density n^* ($n^* = n\sigma^3$) along two isotherms [$T^* = T/(\epsilon/k)$]. Dots represent MD results from Ref. 10, the solid line represents first order perturbation theory at $T^* = 0.5875$, the dashed line represents first order perturbation theory at $T^* = 0.8125$.

for two subcritical isotherms, obtained from theory and from simulation. Table VIII shows the results of the model. This disagreement comes from the wrong values of A_1 obtained at high densities. The contribution of A_1 to the pressure is always negative and proportional to the slope A_1 with the density (see Fig. 2). As the theoretical slope of A_1 is smaller than the true one (in absolute value) the zero pressure densities of the theory are smaller than the true ones. The zero pressure densities obtained from RHNC are smaller than the ones from PY. In any case, the agreement between theory and experiment is modest. Because we saw that the reference system is correctly described by the theory, the origin of the discrepancy is again the wrong values of A_1 at high densities. Keeping in mind that A_1 is wrong due to the fact that the orientational dependence of $y_0(r_{12}, \omega_1, \omega_2)$ is neglected in the theory [see Eq. (27)], we can conclude that for Kihara fluids the proposed perturbation theory always gives smaller densities at zero pressure than it should due to the use of Eq. (27). In Fig. 3, we plot the pressure against the density for the studied model of propane at two different temperatures. We show the theoretical and the MD results. PT overestimates the pressure of the model at the two studied temperatures, and the deviations increase with the density.

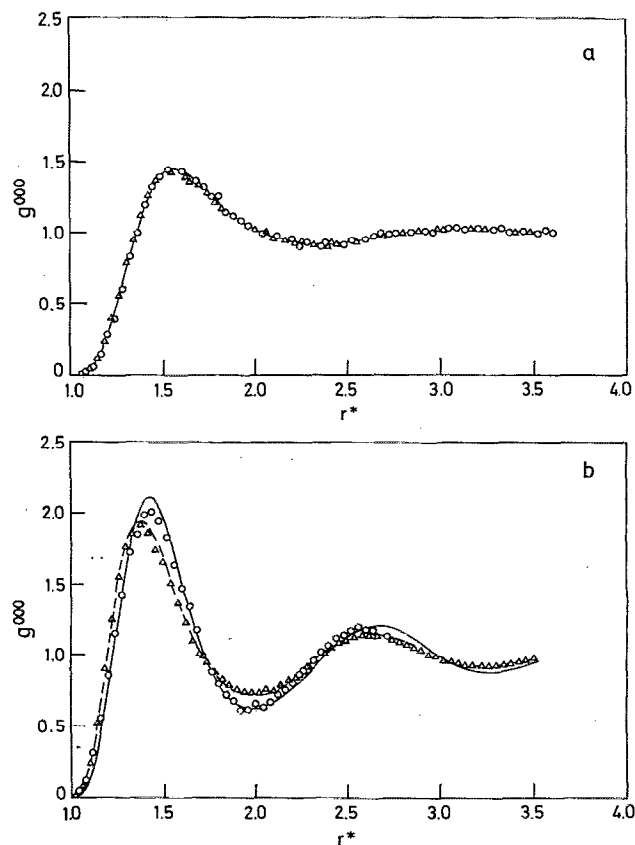


FIG. 4. Radial distribution function for the reference system of the Kihara model of propane as a function of the center of mass separation $r^* = r_{12}/\sigma$. Dots correspond to MD results for the anisotropic reference system from Ref. 10, the solid line corresponds to G_{RAM}^{PY} , the dashed line is G_{RAM} , and (crosses) are MC results of the spherical potential Φ_{RAM} . (a) $T^* = 0.5875$ and $n^* = 0.20$. (b) $T^* = 0.5875$ and $n^* = 0.41$.

TABLE IX. Potential parameters of the Kihara model of propane (Fig. 1) as obtained from MD (Ref. 10) for a given value of L^* and from PT for two values of L^* .

	λ /degrees	L^*	σ/A	ϵ/k
MD ^a	109.5	0.4123	3.6095	398.5
PT1	109.5	0.4123	3.5587	427.
PT2	109.5	0.460	3.4757	438.2

^aReference 10.

Finally, let us see whether the radial distribution function of the reference system is well described by Eqs. (28) and (29). For that purpose, a comparison is shown in Fig. 4 between the MD values of $G_0(r_{12})$ for the reference system¹⁰ and the values of $G_{RAM}(r_{12})$ as given by PY and RHNC solution of the OZ equation for $\Phi_{RAM}(r_{12})$. At low densities [Fig. 4(a)] PY and RHNC agree each other and agree with the results of the MD very well. This is expected because Eq. (28) is exact at zero densities. However, at high densities [Fig. 4(b)] neither PY nor RHNC agree with MD results, showing that Eq. (28) not only gives wrong orientational dependence of $g_0(r_{12}, \omega_1, \omega_2)$, but it is not even able to yield an accurate estimation of the radial distribution function. RHNC describes better the radial distribution function of the reference system at small values of r_{12} , whereas PY describes better the first peak and the behavior at large r_{12} . We also show in Fig. 4 the values of $G_{RAM}(r_{12})$ as obtained from Monte Carlo (MC) of the RAM spherical potential (see Ref. 13 for details). RHNC agrees perfectly with the MC results at low and high densities while PY fails at high densities. It is interesting to note that the theoretical values of A_1 (PY or RHNC) are very close to each other and far away from the exact MD value (see Table VI) in spite of the fact that the structure predicted by these two approaches differs considerably at high densities. This indicates that the only

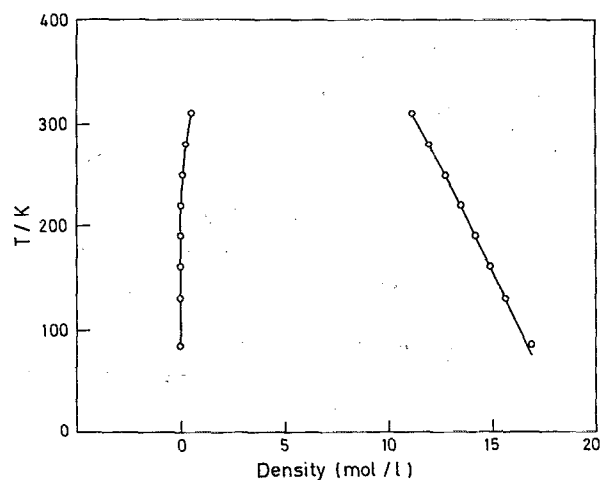


FIG. 5. Densities of propane at the coexistence line. The solid line corresponds to experimental results from Ref. 39 and crosses are the results obtained from second order PT with the potential parameters PT1 of Table IX of this work.

way to obtain more negative estimates of A_1 is to give more orientational dependence to $y_0(r_{12}, \omega_1, \omega_2)$ and not too much can be expected if one continues making spherical approximations to $y_0(r_{12}, \omega_1, \omega_2)$.

V. THEORY VS EXPERIMENT

In the previous section we have tested the different approximations of the theory. We have shown that Eq. (27) introduces a severe error which affects the determination of A_1 in an important way. However, as the error is systematic there is still the possibility to use potential parameters which compensate to some extent these failures. In this way the potential parameters somewhat lose their physical meaning, but the prediction of experimental properties of real substances can be still done in a fast and easy way. This proce-

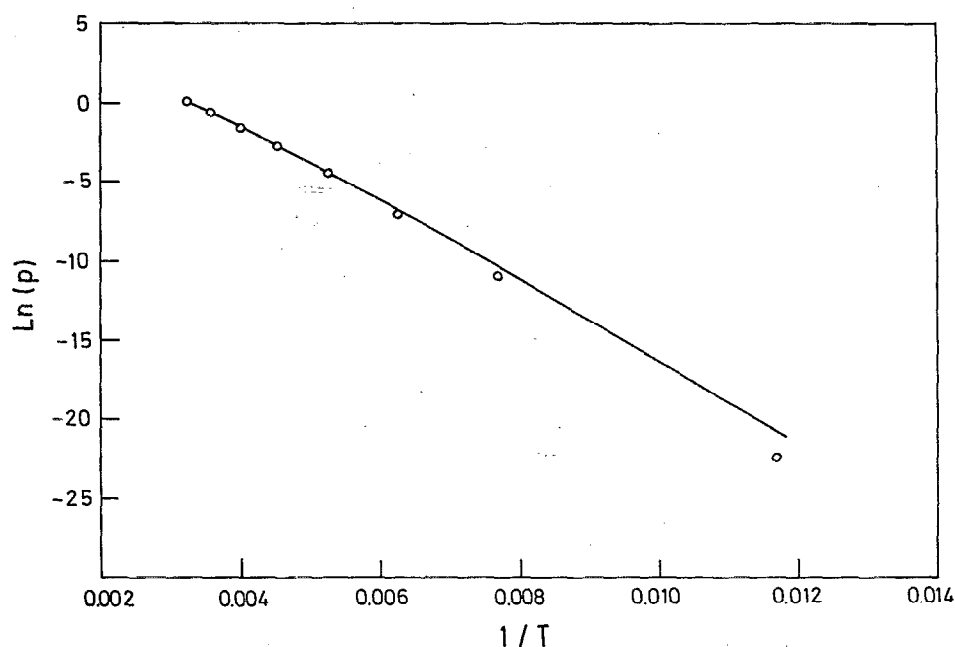


FIG. 6. Logarithm of the vapor pressure of propane (in MPa) as a function of the inverse of the temperature (in K). Dots are experimental results, the solid line represents the theoretical results from second order perturbation theory with potential parameters PT1 of Table IX, and the dashed line correspond to theoretical values from second order perturbation theory with the potential parameters PT2 of Table IX. These two lines are only distinct at high temperatures at the scale of the figure.

ture has already been used by Lustig,⁴ Fischer *et al.*,³⁶ and Kantor *et al.*³⁷ who found the potential parameters of real substances by fitting the theoretical predictions to the experimental results. In this way the potential parameters compensate for the errors which arise from using approximate theories. In this section, we shall show that the PT of Sec. II applied to the Kihara model is able to reproduce the properties of propane within experimental accuracy, as long as the parameters of the potential are fitted to experimental results.

In order to determine the potential parameters we shall fit the theoretical values of orthobaric density and vapor pressure to the experimental ones of propane³⁸ at a given

TABLE X. Vapor-liquid equilibrium of propane as obtained from second order PT with the parameters of Table IX (PT1 and PT2). We also show the experimental results from Ref. 38.

Vapor pressures			
$T/(K)$	$p^{\text{exp}}/(MPa)$	$p^{\text{PT1}}/(MPa)$	$p^{\text{PT2}}/(MPa)$
85.47	1.69×10^{-9}	9.27×10^{-10}	9.15×10^{-10}
130.	1.75×10^{-5}	3.25×10^{-5}	3.27×10^{-5}
160.	8.47×10^{-4}	1.13×10^{-3}	1.14×10^{-3}
190.	1.05×10^{-2}	1.15×10^{-2}	1.17×10^{-2}
220.	6.05×10^{-2}	5.98×10^{-2}	6.10×10^{-2}
250.	0.218	0.189	0.206
280.	0.582	0.516	0.529
310.	1.27	1.10	0.914

Orthobaric densities			
$T/(K)$	$n^{\text{exp}}/(\text{mol}/\ell)$	$n^{\text{PT1}}/(\text{mol}/\ell)$	$n^{\text{PT2}}/(\text{mol}/\ell)$
85.47	16.63	16.86	16.97
130.	15.60	15.62	15.68
160.	14.91	14.86	14.92
190.	14.20	14.14	14.19
220.	13.46	13.43	13.46
250.	12.66	12.70	12.71
280.	11.77	11.94	11.93
310.	10.72	11.13	11.03

Dew densities			
$T/(K)$	$n^{\text{exp}}/(\text{mol}/\ell)$	$n^{\text{PT1}}/(\text{mol}/\ell)$	$n^{\text{PT2}}/(\text{mol}/\ell)$
85.47	2.38×10^{-10}	1.30×10^{-9}	1.29×10^{-9}
130.	1.62×10^{-5}	3.01×10^{-5}	3.03×10^{-5}
160.	6.37×10^{-4}	8.48×10^{-4}	8.59×10^{-4}
190.	6.70×10^{-3}	7.36×10^{-3}	7.44×10^{-3}
220.	3.39×10^{-2}	3.35×10^{-2}	3.42×10^{-2}
250.	0.112	9.11×10^{-2}	0.105
280.	0.289	0.249	0.256
310.	0.635	0.525	0.355

Enthalpy of vaporization			
$T/(K)$	$H_v^{\text{exp}}/(\text{KJ}/\text{mol})$	$H_v^{\text{PT1}}/(\text{KJ}/\text{mol})$	$H_v^{\text{PT2}}/(\text{KJ}/\text{mol})$
110	24.17	22.26	22.32
130	22.96	21.16	21.21
160	21.70	20.15	20.23
190	20.52	19.19	19.26
220	19.26	18.18	18.23
250	17.82	17.06	17.05
280	16.07	15.70	15.65
310	13.76	14.06	13.95

TABLE XI. Second virial coefficient of propane obtained from the parameters of Table IX along with the experimental results (Ref. 41).

$T/(K)$	$B_2^{\text{exp}}/(\text{cm}^3/\text{mol})$	$B_2^{\text{PT1}}/(\text{cm}^3/\text{mol})$	$B_2^{\text{PT2}}/(\text{cm}^3/\text{mol})$
85.47	...	-10 526	-11 542
130.	...	-2465	-2593
160.	...	-1435	-1491
190.	...	-967	-996
220.	-763 ± 30	-707	-724
250.	-571 ± 20	-544	-555
280.	-445 ± 20	-433	-441
310.	-357 ± 10	-353	-359

temperature. We choose an intermediate temperature between the triple point and 0.8 times the critical temperature of propane. All the calculations of this section were done by using second order PT, the Boublik EOS with α obtained from B_{2H} and $\gamma_{\text{RAM}}^{\text{PV}}$.

The value of the internal angle of the angular model was fixed to 109.5 deg. Two values of the reduced length of the rod $L^* = l/\sigma$ with l being the length of the rod were considered $L^* = 0.4123$ and $L^* = 0.46$. In Table IX the obtained parameters with the theory are shown along with the parameters obtained from MD¹⁰ for $L^* = 0.4123$ using the fitting procedure of Ref. 39. We observe that for $L^* = 0.4123$ MD parameters are not coincident with those of PT. In fact, PT gets a slightly smaller molecular volume (smaller value of σ) and increases the value of ϵ/k . Thus the errors of the theory affects 2% to σ and 7% to ϵ/k . The variation with L^* of the theoretical σ tends to keep constant the molecular volume. The theoretical ϵ/k increases with L^* .

In Fig. 5 we represent the vapor-liquid equilibrium of propane. The agreement in the coexistence densities is excellent. In Fig. 6 the vapor pressure is plotted at different temperatures. The agreement is very good at intermediate temperatures and slightly deteriorates at low temperatures. Table X gives a more detailed panorama of the vapor-liquid equilibria of propane. Table X also shows the calculated enthalpy of vaporization H_v at several temperatures along with the experimental results.³⁸ The deviations in H_v go from 8% at the lowest temperature to 2% at the highest. Finally, in Table XI we compare theoretical and experimental values of B_2 for propane.⁴⁰ The agreement is also good. Thus, we see from our results that the vapor-liquid equilibria of an angular, nonpolar molecule as propane can be well described by the proposed PT when the potential parameters are obtained by fitting the theoretical to the experimental results.

VI. CONCLUSIONS

In a previous work¹⁰ we show that the simulation by MD of angular Kihara fluids is easy to carry out. Furthermore, we show that the Kihara model can compete as effective pair potential with the site-site model for angular, nonpolar substances as propane. Moreover, the WCA-like division of the pair potential can be easily done for this model and, therefore, the simulation of the reference system is really feasible while it is very difficult for a site-site model. Simulations of the reference system indeed were carried out, al-

lowing the evaluation during the runs of the different perturbation terms.

In this work we have carried out an extension of the perturbation scheme proposed by Fischer, to Kihara angular models. Furthermore, a systematic study of the different approximations of the theory has been made by comparing the pseudoexperimental MD results with the theoretical ones. This study revealed that the reference system is well described by Boublik EOS with α obtained from B_{2n} . Nevertheless, the main shortcoming of the PT is to neglect the orientational dependence of $y_0(r_{12}, \omega_1, \omega_2)$ [Eq. (27)]. Although this approximation is good at low densities, it fails at high densities giving theoretical estimates of A_1 less negative than they should be. Therefore, the pressure is over predicted at high densities. Not too much can be won by using the accurate $y_{\text{RAM}}^{\text{RHNC}}(r_{12})$ [when compared with MC structural results corresponding to the $\Phi_{\text{RAM}}(r_{12})$] instead of the approximate $y_{\text{RAM}}^{\text{PY}}(r_{12})$. Only with incorporating more orientational dependence on $y_0(r_{12}, \omega_1, \omega_2)$ can a better description of A_1 be expected. Efforts to improve the theory should address this point. First order PT should be enough at high densities but, at low and medium densities second order PT should be used. The macroscopic compressibility approximation serves reasonably well to estimate A_2 .

We have also shown that the potential parameters obtained from an approximate theory can differ from the parameters obtained from a simulation study as MD. In this way the potential parameters obtained from the theory compensate to some extent the errors of the theory. Thus, a good description of real propane is achieved with the proposed PT when the potential parameters are obtained by fitting theoretical to experimental results. The agreement was similar to the one obtained by PT and the site-site model.⁴

We believe that the Kihara model can be used to model the pair interaction of small nonpolar molecules (linear and nonlinear), either by simulation studies (see Ref. 10) or by PT, as we showed in this work. The difficulties to carry out such studies are not greater than with the site-site model. Moreover, systematic improvement of the theory can be achieved because the simulation of the WCA-like reference system is easy to carry out whereas this is not true for the site-site model.

ACKNOWLEDGMENTS

This work was financially supported by Project PB88-0143 of the Dirección General de Investigación Científica y Técnica. One of us (C.V.) is grateful for a grant from the Plan de Formación de Personal Investigador.

APPENDIX

In this Appendix we shall give the basic formulas to evaluate R_H , S_H , and V_H for a hard molecule made up by two identical, fused hard spherocylinders as shown in Fig. 1. We shall call λ the internal angle between the rods and we shall consider only models with $\lambda > \pi/2$ and $L^* = l/\sigma > 0.5/\text{tg}(\lambda/2)$. For R_H we shall take the mean radius of curvature of the parallel body of width $\sigma/2$ to the

triangle made up by the two rods. Then R_H is given by⁴¹

$$R_H = \frac{3}{8} \bar{l} + \frac{\sigma}{2}, \quad (\text{A1})$$

where \bar{l} is the average length of the side of the triangle

$$\bar{l} = \frac{(l_1 + l_2 + l_3)}{3}, \quad (\text{A2})$$

l_1 , l_2 , and l_3 denoting the length of the sides of the triangle.

To evaluate the surface S_H and the volume V_H , we write them as

$$X_H = X_1 + X_2 - X_{12}, \quad (\text{A3})$$

where X_i stands for the value of property X for spherocylinder i and X_{ij} stands for the value of the property in the region common to spherocylinders i and j with $X = S, V$. The values of S_i and V_i are trivial and are given by

$$S_i = \pi \sigma^2 (1 + L^*) \quad (\text{A4})$$

$$V_i = \frac{\pi}{6} \sigma^3 \left(1 + \frac{3}{2} L^* \right). \quad (\text{A5})$$

To evaluate X_{ij} we shall divide the common region into two parts, a spherical sector (labeled II in Fig. 1) and a cylindrical one (labeled III in Fig. 1). The contribution of sector II to X_{ij} is trivial and is given by

$$S_{ij}^{\text{II}} = \sigma^2 (\pi + \lambda) / 2 \quad (\text{A6})$$

$$V_{ij}^{\text{II}} = \sigma^3 (\pi + \lambda) / 12. \quad (\text{A7})$$

The contribution of sector III to X_{ij} can be evaluated from integration to yield

$$S_{ij}^{\text{III}} = \frac{\pi \sigma^2}{4 \text{tg}(\lambda/2)} \quad (\text{A8})$$

$$V_{ij}^{\text{III}} = \frac{\sigma^3}{6} \cotg(\lambda/2). \quad (\text{A9})$$

Equations (A1) to (A9) allow to evaluate α from geometrical considerations for the studied model very easily.

¹S. Gupta, J. Yang, and N. R. Kestner, *J. Chem. Phys.* **89**, 3733 (1988).

²R. Lustig and W. Steele, *Mol. Phys.* **65**, 475 (1988).

³S. Toxvaerd, *J. Chem. Phys.* **91**, 3716 (1989).

⁴R. Lustig, *Mol. Phys.* **59**, 173 (1986).

⁵J. Fischer, *J. Chem. Phys.* **72**, 5371 (1980).

⁶J. D. Weeks, D. Chandler, and H. C. Andersen, *J. Chem. Phys.* **54**, 5237 (1971).

⁷T. Kihara, *J. Phys. Soc. Jpn.* **16**, 289 (1951).

⁸R. K. Kantor and T. Boublik, *Czech. J. Phys. B* **38**, 321 (1988).

⁹C. Vega and D. Frenkel, *Mol. Phys.* **67**, 633 (1989).

¹⁰C. Vega and S. Lago, *J. Chem. Phys.* **93**, 8171 (1990).

¹¹P. Padilla and S. Lago, *Fluid Phase Equilibria* **48**, 53 (1989).

¹²T. Boublik, *J. Chem. Phys.* **87**, 1751 (1988).

¹³C. Vega and S. Lago, *Mol. Phys.* (in press).

¹⁴K. C. Mo and K. E. Gubbins, *Chem. Phys. Lett.* **27**, 144 (1974).

¹⁵J. P. Hansen, I. R. McDonald, *Theory of Simple Liquids*, 2nd ed. (Academic, New York, 1986).

¹⁶C. G. Gray and K. E. Gubbins, *Theory of Molecular Fluids* (Clarendon, Oxford, 1984).

¹⁷T. Boublik and I. Nezbeda, *Coll. Czech. Chem. Commun.* **51**, 2301 (1986).

¹⁸T. Boublik, *J. Chem. Phys.* **63**, 4084 (1975).

¹⁹I. Nezbeda, *Chem. Phys. Lett.* **41**, 55 (1976).

²⁰T. Boublik, *Mol. Phys.* **42**, 209 (1981).

²¹H. Hadwiger, *Altes und Neues über konvexe Körper* (Birkhauser, Basel, 1955).

²²M. Rigby, *Mol. Phys.* **32**, 575 (1976).

²³F. Lado, *Mol. Phys.* **47**, 283 (1982).

- ²⁴S. Lago and P. Sevilla, *J. Chem. Phys.* **89**, 4349 (1988).
²⁵A. Perera and G. N. Patey, *J. Chem. Phys.* **89**, 5681 (1988).
²⁶L. J. Lowden and D. Chandler, *J. Chem. Phys.* **61**, 5228 (1974).
²⁷B. J. Berne and P. Pechukas, *J. Chem. Phys.* **56**, 4213 (1972).
²⁸F. Lado, *Phys. Lett. A* **89**, 196 (1982).
²⁹T. Boublik, I. Nezbeda, and K. Hlavaty, *Statistical Thermodynamics of Simple Liquids and Their Mixtures* (Academia, Praha, 1980).
³⁰H. Conroy, *J. Chem. Phys.* **47**, 5307 (1967).
³¹P. Sevilla and S. Lago, *Comput. Chem.* **9**, 39 (1985).
³²S. Lago and C. Vega, *Comput. Chem.* **12**, 343 (1988).
³³S. Labik, P. Malijevsky, and P. Voňka, *Mol. Phys.* **56**, 709 (1985).
³⁴A. Malijevsky and S. Labik, *Mol. Phys.* **60**, 663 (1987).
³⁵S. Labik and A. Malijevsky, *Mol. Phys.* **67**, 431 (1989).
³⁶J. Fischer, R. Lustig, H. Breitenfelder-Manske, and W. Lemming, *Mol. Phys.* **52**, 485 (1984).
³⁷R. Kantor and T. Boublik, *Ber. Bunsenges. Phys. Chem.* **92**, 1123 (1988).
³⁸R. D. Goodwin and W. M. Haynes, *Natl. Bur. Stand. (U.S.) Monograph* **170** (1982).
³⁹C. Vega, B. Saager, and J. Fischer, *Mol. Phys.* **68**, 1079 (1989).
⁴⁰J. H. Dymond, J. A. Cholinski, A. Szafranski, and D. Wyrzykowska-Stankiewicz, *Fluid Phase Equilibria* **27**, 1 (1986).
⁴¹R. Lustig, *Mol. Phys.* **59**, 195 (1986).